17th World Conference on Earthquake Engineering, 17WCEE
Sendai, Japan - September 13th to 18th 2020

TOWARDS THE STRONG MOTION FLATFILE IN CHINA: CONCEPT AND PURPOSE

Y.F. Ren[(1)], X.X. Yao[(2)], T. Kishida[(3)], R.Z. Wen[(4)], P.B. Xu[(5)], K. Ji[(6)], S. Midorikawa[(7)], H.J. Si[(8)], H.W. Wang[(9)], Y.T. Zhang[(10)]

[(1)] *Professor, Institute of Engineering Mechanics, China Earthquake Administration, renyefei@iem.net.cn*
[(2)] *PhD candidate, Institute of Engineering Mechanics, China Earthquake Administration, yaoxinxiniem@126.com*
[(3)] *Assistant professor, Khalifa University of Science and Technology, tadahiro.kishida@ku.ac.ae*
[(4)] *Professor, Institute of Engineering Mechanics, China Earthquake Administration, ruizhi@iem.ac.cn*
[(5)] *PhD, Institute of Engineering Mechanics, China Earthquake Administration, xupeibin13@126.com*
[(6)] *Assistant professor, Institute of Engineering Mechanics, China Earthquake Administration, jikun@iem.ac.cn*
[(7)] *Professor Emeritus, Tokyo Institute of Technology, smidorik21@gmail.com*
[(8)] *Visiting Research Fellow, University of Tokyo, shj@eri.u-tokyo.ac.jp*
[(9)] *Assistant professor, Institute of Engineering Mechanics, China Earthquake Administration, whw1990413@163.com*
[(10)] *Postgraduate, Institute of Engineering Mechanics, China Earthquake Administration, 2582622168@qq.com*

Abstract

As we know many countries in the world have updated the technology of strong motion observation and improved the capability of network monitoring, that facilitates the amount of global ground motion records growing in a fantastic speed. The accumulation of strong motion records accelerates the development of earthquake engineering, e.g., a bloom of ground motion prediction equation (GMPE) in recent years. For the sake of being used conveniently and extensively, the strong motion records will be assembled to compile a flatfile which will be released freely in public. Generally, the strong motion flatfile is a parametric table which contains the information of earthquake source and station site, source-to-site distance metrics and processed ground motion intensity measures. There are several strong motion flatfiles have been used popularly in the world, e.g., flatfile of NGA-West2 global strong motion database, flatfile of KiK-net strong motion data, flatfile of pan-European engineering strong motion.

The China Strong Motion Network Center (CSMNC) has collected about 12, 200 strong motion records in 2270 earthquake events during the time from 2007 to 2018, including M_S 8.0 Great Wenchuan Earthquake and M_S 7.0 Lushan Earthquake. However, these data have not been well proofed and they are deficient in data processing. Some fundamental information such like earthquake magnitude has not been manually checked and the site condition of strong motion stations not essentially provided. In this regard, the main objective of this paper is to develop a flatfile of Chinese strong ground motion preliminarily. Firstly, the architecture of this flatfile will be introduced as well as the standard of data compile. Secondly, all the information related to records, stations and earthquakes will be checked essentially one-by-one to remove the man-made errors. For instance, the locations or name codes of some stations are amended but not be reported, the information of some stations is inaccuracy, such as longitude, latitude, site condition, et al, and the issued three components (EW, NS and UD) are actually disordered at some stations.

Moreover, data processing is a vital step in developing the strong motion flatfile. Its flowchart will be designed in order to seek an optimal value of corner frequency of high-pass filtering, considering the criteria including (1) low-frequency Fourier amplitude spectrum match with the w^2 source model, (2) the signal-to-noise-ratio (SNR) should be larger than 3, (3) the displacement within the noise window is checked to be zero after causal filter to ensure that usable bandwidth is not contaminated by noise, and (4) assuring velocity and displacement time-histories appear to physical after acausal filter which indicates the corner frequency is advisable. The earthquake source information will be reviewed individually based on the seismic catalog provided by China Earthquake Network Center. The focal mechanism for large events will be derived from the GCMT or published literatures and the empirical method will be used for small events. The site database will be built based on three considerations, borehole data is prior if available, empirical relationship between site class and H/V spectral ratio are second option if strong motion records are available, and empirical model between site parameters and geological or topographic proxies is the last choice.

Keywords: Strong motion flatfile; Chinese strong motion record; Data processing; Site database

1. Introduction

The strong motion observation plays an important role on the earthquake engineering community presently. For the sake of scientific research, the recorded waveforms are usually used as the basic dataset for developing new empirical models, recognizing new knowledge on ground motion, etc., as they reflect the nature of the source, propagation path and local site effects. For the sake of engineering practice, the recorded waveforms are usually used as the input of earthquake excitation in the structural dynamic time-history analysis, as they are retrieved from a real earthquake event. Regarding the numerous demands for public use, compiling a flatfile for the observed strong ground motions is urgently needed, that commonly includes parameters relating to the earthquake source and station site, source-to-site distance metrics and processed ground motion intensity measures. There are several strong motion flatfiles have been used popularly in the world, e.g., flatfile of NGA-West2 global strong motion database [1], flatfile of KiK-net strong motion data [2], and flatfile of pan-European engineering strong motion [3], but not for the Chinese ground motions.

In 2008, the new-generation National Strong Motion Observation Network System (NSMONS) in China was established as a part of the National 10th Five-Year Plan (2001-2005). This network consisted of 1154 permanent free-field strong motion stations, 310 intensity stations, 5 data centers, 10 special structural arrays, and 5 storage arrays. Strong motion stations were mainly installed in 21 key-areas for earthquake surveillance to enhance the ability of earthquake monitoring and the collection of strong motion records in the most seismically active regions and some major cities in the Chinese mainland [4]. The NSMONS retrieved a large number of strong motion records, especially in some large events, such as 2008 M_s8.0 Wenchuan Earthquake, 2013 M_s7.0 Lushan Earthquake. Although the data has been used in many studies, such as spectral property inversion [5], correlation of spectrum intensities [6], single-station standard deviation analysis [7] and others, the data is mainly disseminated domestically. One of the most important reasons is lack of supplementary source and site information released by an authority. The complete lists including source, path, site information only can be found for the typical destructive earthquakes, such as 2008 M_s8.0 Wenchuan Earthquake [1, 8], 2013 M_s7.0 Lushan Earthquake [9, 10] and 2017 M_s7.0 Jiuzhaigou Earthquake [11].

Towards the strong motion flatfile in china, this paper will present firstly an overview of the collected strong ground motions in China since from 2007 to 2018. Then the architecture of this flatfile will be introduced briefly as well as the standard of data compile. Secondly, a flowchart of high-pass filtering will be designed in order to seek an optimal value of corner frequency, considering some specific rules record-by-record. Three schemes used to build the site database are suggested finally, i.e., borehole data is prior if available, empirical relationship between site class and H/V spectral ratio is the second option if strong motion records are available, and empirical model between site parameters and geological or topographic proxies is the last choice.

2. Overview of the Collected Strong Motion Data

The NSMONS started be in trial operation in 2007. It collected ~12, 000 strong motion recordings since from 2007 to 2018. Table 1 shows the numbers of recordings for each issue released in public by NSMONS. Before 2007 the NSMONS released 11 issues of recordings which were retrieved by the analogue instruments. Due to poor quality of most ones, e.g., missing P wave as well as low amplitude, this study excludes these recordings.

All the data were recorded in ~900 earthquakes, most of which are small events with magnitude less than 6.0, as shown in Fig.1(a). The epicentral distance covers a range of 1 km to 1,000 km, supporting for investigating the regional attenuation property of ground motion. There are only a few of data of which the peak ground acceleration (PGA) are larger than 100 cm/s^2. Almost ~1000 recordings are retrieved from the events with magnitude larger than 6.0. These data will have great contributions on the studies that rely on the observed ground motions, such as developing a regional ground motion model (GMM).

Table 1 – Issues of strong motion recordings released by NSMONS since from 2007 to 2018 and numbers of recordings for each issue

Issue	Description	Numbers of Rec.
12	Wenchuan mainshock	430
13	Wenchuan aftershocks at permanent stations	2030
14	Wenchuan aftershocks at temporary stations	2214
15	Other earthquakes from 2007 to 2009	833
16	Other earthquakes from 2010 to 2011	682
17	Lushan earthquake sequence	1243
18	Other earthquakes from 2012 to 2013	1474
19	Other earthquakes from 2014 to 2015	1987
-	Earthquakes from 2016 to 2018	1268
Total		12161

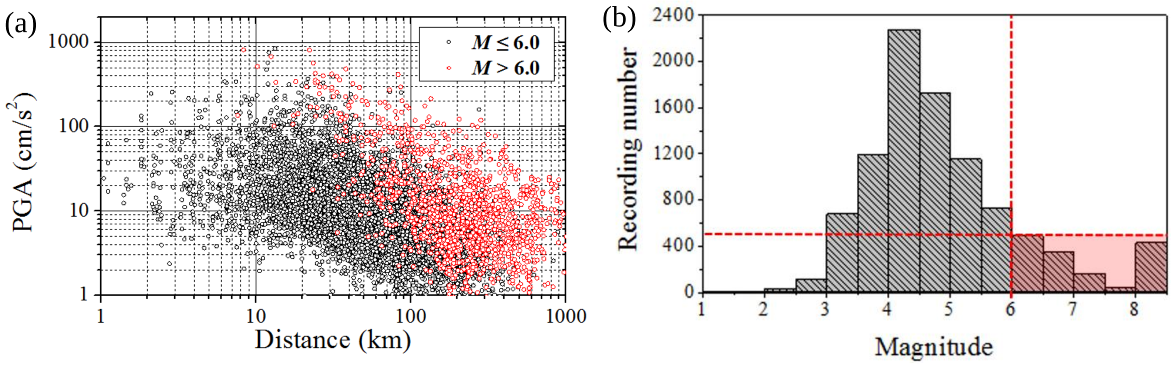

Fig. 1 – (a) PGA versus epicentral distance for strong motion recordings collected by NSMONS since from 2007 to 2018. (b) Histograms of recordings obtained in earthquakes with different magnitudes. The red lines and shaded area highlight the recording numbers counting in the events with magnitude larger than 6.0.

Table 2 shows a list of 15 earthquakes with magnitude larger than 6.0 occurred in Chinese mainland since 2008 and the number of retrieved strong motion recordings in each event. Some highlights derived from these recordings could be summarized as follows: (1) all these earthquakes occurred in the western part of China; (2) there are four event with magnitude larger than 7.0, i.e., Wenchuan earthquake, Yushu earthquake, Lushan earthquake and Jiuzhaigou earthquake; (3) the considerable amounts of recordings are obtained in some large events, particularly in Wenchuan (420), Lushan (121), Ludian (79) and Jiuzhaigou (66) earthquakes; (4) the maximum recording in the history of China were captured at Baoxing station with PGA larger than 1g in the Lushan earthquake; (5) the near-fault effects on the observed ground motions are revealed significantly, such as the rupture directivity effect in Wenchuan earthquake [12] and hanging/foot wall effect in the Lushan earthquake [9]; (6) it seems that these data support us adequately to develop a local GMM for Chinese mainland.

Table 2 – The earthquake list for its magnitude larger than 6.0 in Chinese mainland since 2008 and the number of strong motion recordings retrieved in each event

EQ name	Date of EQ	M_S	Numbers of Rec.
Wenchuan	May 12, 2008	8.0	420
Yushu	April 14, 2010	7.1	5
Yili	November 1, 2011	6.0	8
Xinyuan	June 30, 2012	6.6	33
Lushan	April 20, 2013	7.0	121
Minxian	July 22, 2013	6.7	64
Yingjiang	May 30, 2014	6.1	11
Ludian	August 3, 2014	6.5	79
Jinggu	October 7, 2014	6.6	39
Kangding	November 22, 2014	6.4	55
Pishan	July 3, 2015	6.5	39
Aketao	November 25, 2016	6.7	33
Hutubi	December 8, 2016	6.2	37
Jiuzhaigou	August 8, 2017	7.0	66
Jinghe	August 9, 2017	6.6	17

3. Architecture of strong motion flatfile

To meet the various needs of all data users, it is suggested that the strong motion flatfile contains the related information as comprehensive as possible. In our work, we consider six categories of data, including parameters or flags related to event, source, station, source-to-site distance, waveform and intensity measures (IMs). The details of each category are descripted in the following:

(1) The event-related metadata includes the event ID, time and name, epicenter longitude and latitude, focal depth, flag of main shock or aftershock, M_W, M_S and M_L.

(2) The source-related metadata includes the fault type, rupture strike, dip and rake, depth to the top of rupture plane (Z_{tor}).

(3) The station-related metadata includes the station name and code, location longitude and latitude, site class, V_{S30}, and flags representing the ways to determine site class and V_{S30} by either measured or predicted. The predicted methods will be descripted in the following section 5.

(4) The metrics of source-to-site distance includes the epicenter distance, hypocenter distance, Joyner-Boore distance (the closest distance to the surface projection of fault rupture plane) and rupture distance (the closest distance to the fault rupture plane).

(5) The waveform metadata includes the time interval of data sampling, waveform duration, channel code, corner frequency of high-pass filtering (f_{hp}) and corner frequency of low-pass filtering (f_{lp}). The way how to seek an optimal value of f_{hp} will be introduced briefly in the following section 4.

(6) The intensity measures include the PGA, peak ground velocity (PGV), peak ground displacement (PGD), cumulative absolute velocity (CAV), Housner intensity (I_H), Arias intensity acceleration (I_A), velocity and displacement response spectral ordinates with 5% damping ratios at 105 oscillation periods from 0.01 to 10 s (S_a, S_v and S_d), 5%–75% significant duration (D_{SR}(5–75%)) and 5%–95% significant duration (D_{SR}(5–95%)). IMs are provided for each record component and in terms of orientation independent values, RotD00, RotD50 and RotD100.

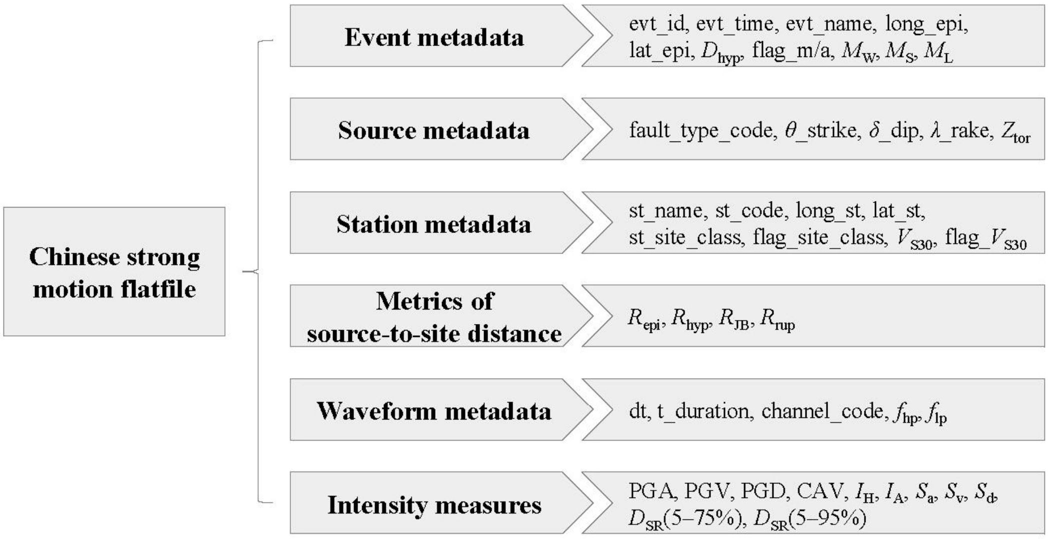

Fig. 2 – Schematic structure of the Chinese strong motion flatfile contents

The designed architecture of our strong motion flatfile is shown in Fig.2. There are some other parameters, such as seismic moment, fault rupture length and width etc., excluded in this flatfile, considering their low frequency of use in the field of earthquake engineering. Note that the numbers of parameters included in this flatfile are much less than those included in NGA-West2 [1]. For saving time due to limited labor capacity, we only choose the most important parameters included and anticipate to update the others in subsequent work.

4. Record Processing

Data processing is a vital step in compiling a strong motion flatfile. Before processing the record, the man-made errors of collected strong motion recordings are check manually, including that the locations or name codes of some stations are updated but not be reported; the information of some stations is inaccuracy, such as longitude, latitude, site condition, et al.; and the issued three components (EW, NS and UD) are actually disordered at some stations. The recordings including these man-made errors should be excluded in order to make sure all information provided by our flatfile are correct as possible as we can.

A recommended value of f_{hp} and f_{lp} will be individually provided in the waveform metadata. For low-pass filtering, f_{lp} is easily evaluated according to the signal-to-noise (SNR) test. For high-pass filtering, f_{hp} is searched for an optimal value component-by-component considering several criteria, including that (1) low-frequency Fourier amplitude spectrum match with the f^2 source model; (2) the SNR should be larger than 3; (3) the displacement within the noise window is checked to be zero after causal filter to ensure that usable bandwidth is not contaminated by noise; (4) assuring velocity and displacement time-histories appear to physical after acausal filter which indicates the corner frequency is advisable. A flowchart including all key steps is illustrated in Fig.3. The procedure and criteria we used in this study are same with those used in NGA-West2 database [1, 13].

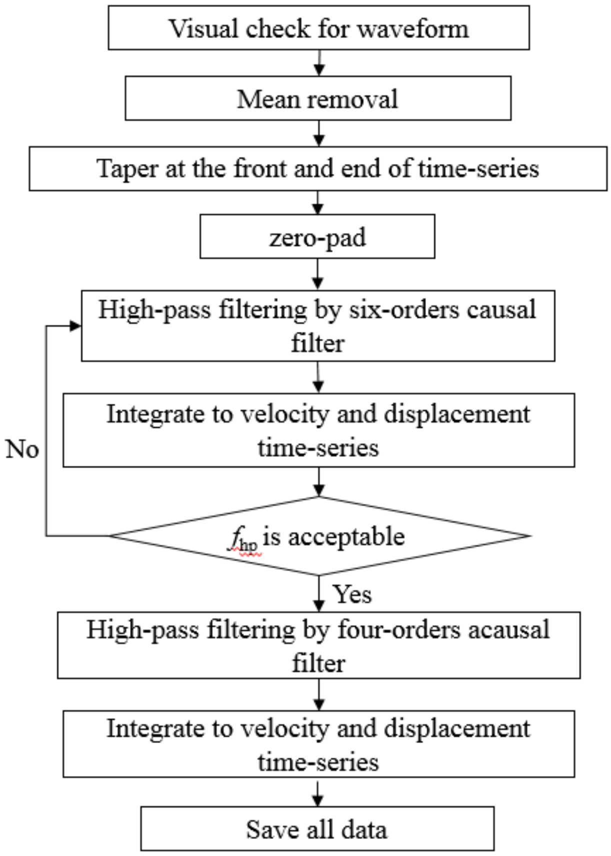

Fig. 3 – Flowchart of high-pass filtering in processing the strong motion recordings of China

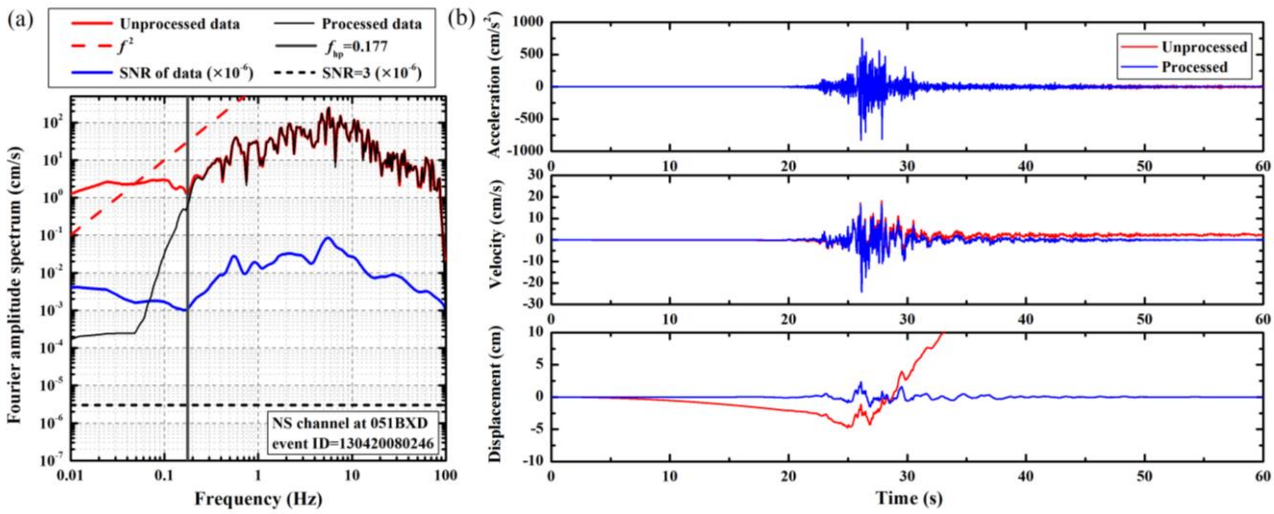

Fig. 4 – (a) A typical case illustrating how to choose an optimal vaule of corner frequency for high-pass filtering. The Fourier amplitude spectrum of raw recording are compared with those calculated by the processed recordings. (b) Comparisons of acceleration, velocity and displacement time-histories of the examplified recording before and after its acausal filtering.

Fig.4 illustrate a typical case showing how to determine an optimal value of f_{hp}. The recording is retrieved in the NS channel at 051BXD station during the Lushan earthquake (event ID is 130420080246). The SNR test shows that the recording meets the criterion (i.e., SNR > 3) covering the entire frequency range of 0.01 Hz – 100 Hz. We determine that 0.177 Hz is acceptable for f_{hp} after causal filtering using this value as a corner frequency. And the integrated velocity and displacement time-histories after acausal filtering appear to physical, which means that the end of waveform trends to be zero, as shown in Fig. 4 (b).

5. Schemes for building site database

As we know the local site effect of near surface could dominate the vibration intensity and frequency of ground motions during the earthquake. The detailed site information is usually requested by data users of strong motion recordings. Therefore, it recommends strongly that a strong motion flatfile should contain a site database. V_{S30} is a parameter included commonly in the site database, sometimes the site class or the site natural period is also a preferred option. The NSMONS provides the site information, only the description of either "rock" or "soil" for each strong motion station. To estimate the value of V_{S30} and site class, three schemes are suggested:

(1) If the borehole data is available, the value of V_{S30} is calculated exactly by the borehole data, as same as for classifying the site class. Until now this study has collected data from ~200 borehole in the vicinity of strong motion stations.

(2) If the borehole data is unavailable, an empirical relationship between site class and H/V spectral ratio (HVSR) is suggested to classify the site class. The details will be explained in the following text.

(3) If the borehole data is unavailable, a proxy-based method will be used to estimate the value of V_{S30}.

Note that the definitions of site class in Chinese code are different with the other country's codes such as the NEHRP and Eurocode 8. Rather than only using V_{S30}, two other parameters are used to define a site class in Chinese code, that are the 20 m equivalent shear wave velocity (V_{S20}) and the thickness of the soil layers (H*) above the engineering bedrock layer where $V_S \geq 500$ m/s, as shown in Table 3. That's the reason why the site class for each strong motion station will be included in this flatfile.

Table 3 Definitions of site classes in the Chinese seismic code (GB50011-2010)

20 m equivalent shear wave velocity V_{S20} (m/s)	**thickness of soil layer H* (m)**				
	I_0	**I**	**II**	**III**	**IV**
> 800	0				
(500，800]		0			
(250，500]		< 5	≥ 5		
(150，250]		< 3	3～50	> 50	
≤150		< 3	3～15	15～80	> 80

H*: thickness of soil layer above engineering rock where $V_S \geq 500$ m/s

5.1 Empirical site classification method

Our previous work [14] proposed an empirical method to classify site class by means of horizontal to-vertical spectral ratio (HVSR) of strong motion recordings. Using the strong-motion recordings and borehole data from KiK-net in Japan, the standard HVSR curves for three site classes (CL-I, CL-II, or CL-III) defined in the Chinese seismic code were suggested, as shown in Fig.5.

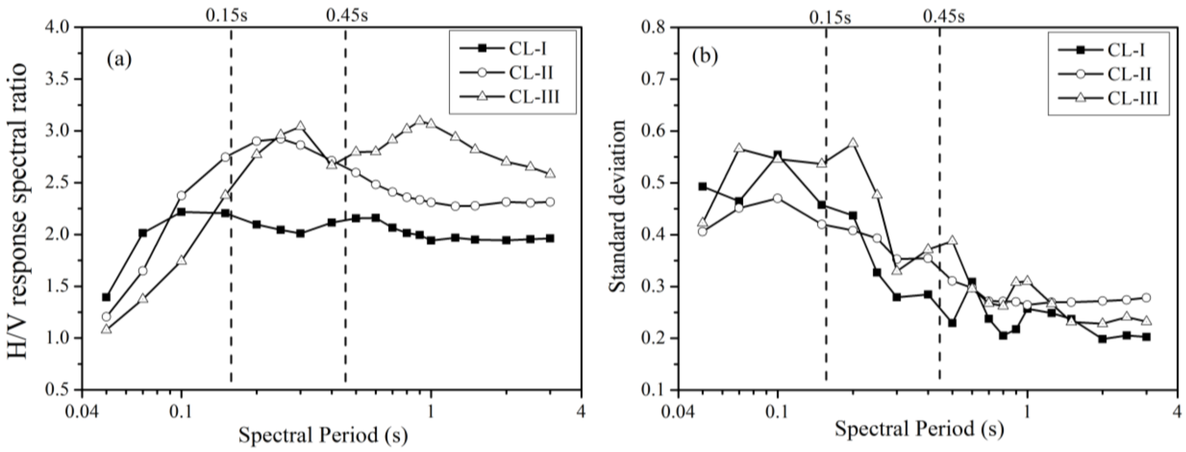

Fig. 5 – (a) Mean HVSR H/V spectral ratios and (b) corresponding standard deviations proposed by [14] for three site classes defined in the Chinese seismic code

Then an empirical site classification scheme was proposed based on comprehensive consideration of peak period, amplitude, and shape of the HVSR curve, as shown in Fig.6, the details of which are explained in the following.

(a) If a curve has more than one peak and if one (or more) of them lies within the range of short periods (< 0.20 s) while the other (or others) lies in the range of long periods (> 0.45 s), this site would be classified ambiguously; therefore, it should be excluded. This aims to avoid any interference in the classification of CL-I sites, some of which have a relatively small T_g. The set period range (0.20 s and 0.45 s) depends on the T_g boundary separating each site class, as shown in Fig. 5(a).

(b) When the amplitude of the HVSR is < 2.0 over the entire period range, the shape of the curve is recognized as relatively flat. The site can be classified directly as belonging to class CL-I.

(c) When T_g is < 0.15 s, the site is classified as CL-II if the peak value is > 4.0 and as CL-I, if < 4.0. This step recognizes that some CL-II sites might have a short predominant period similar to CL-I sites, but that their amplification is usually relatively higher.

(d) As shown in Fig. 5(a), the ranges of T_g for classes CL-II and CL-III partially overlap and the amplitudes of the HVSR curves are partially similar. Therefore, these two classes cannot be classified based simply on their range of predominant period or amplitude. Therefore, for the situation of T_g > 0.15 s, the Spearman's correlation coefficient SI (Eq. (1)) is used to distinguish CL-II and CL-III sites.

$$\mathrm{SI}_k = 1 - 6\sum \frac{d_i^{\,2}}{n(n^2-1)} \tag{1}$$

where d_i is the difference between each rank of corresponding values of the standard HVSR curves for the k-th site class and the target sites, and n is the total number of periods.

(e) After identifying the CL-II and CL-III classes, the significance of the Spearman's correlation coefficients must be checked using a t-distribution hypothesis test at the 0.05 significance level. The testing targets are the mean HVSR of target station and the standard HVSR curve for CL-II or CL-III. If the significant value P is > 0.05, the classification result is considered unacceptable and the station excluded.

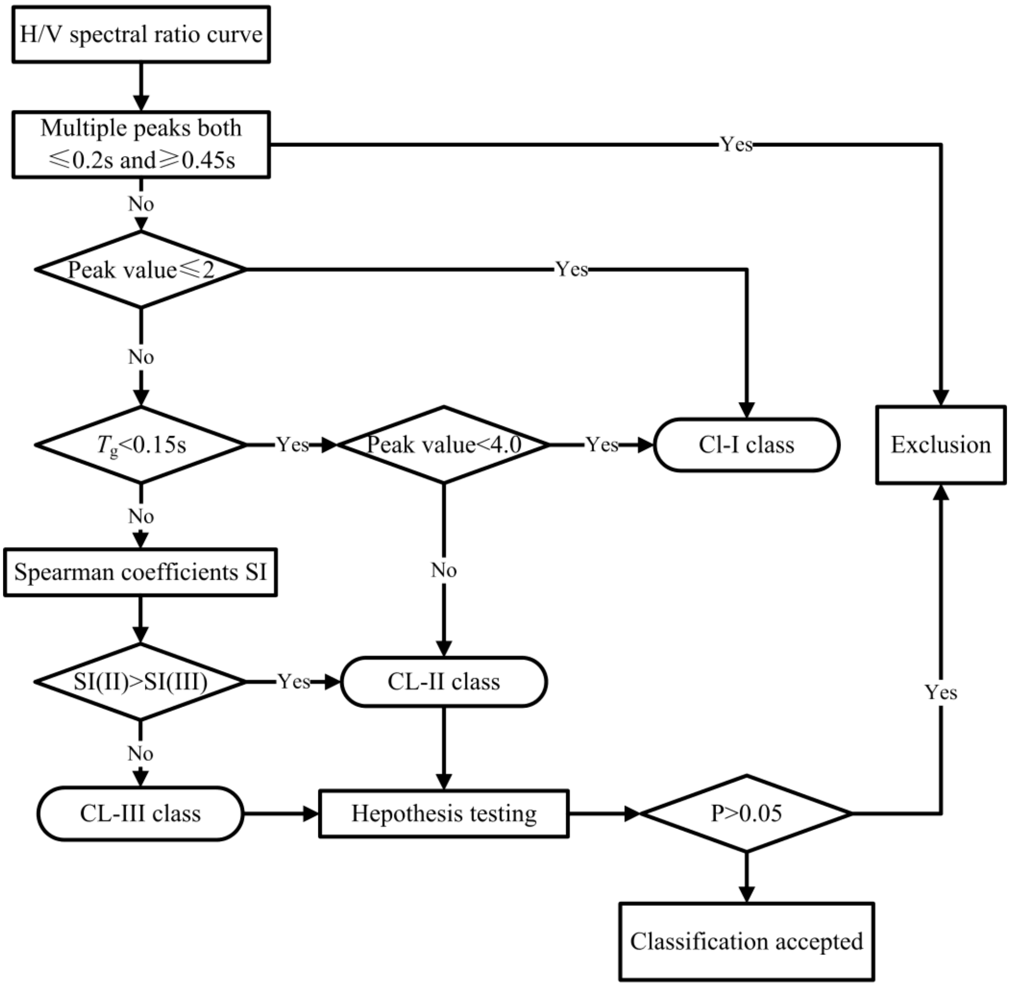

Fig. 6 – Flowchart of proposed empirical HVSR site classification scheme for NSMONS stations

The method was validated that its success rates in identifying CL-I, CL-II, and CL-III sites were 63%, 64%, and 58% respectively. 178 NSMONS stations have been classified their site classes using this method. Regarding more recordings are collected than the study of [14], more stations will be classified their site classes in the next work.

5.2 Proxy-based method for estimating V_{S30}

The proxy-based method has been used popularly used for estimating V_{S30} value at a site in the absence of geophysical measurements. The topographic slope, geologic condition and terrain are three of used popularly proxies, and the empirical relationship between them and V_{S30} have been suggested respectively depending on local data from different countries [15, 16, 17].

We collect borehole data, 30 arc sec topographic data and national surface geology map, and anticipate to develop the proxy relationship with V_{S30} for different region considering its regional dependency. Fig.6 (a) shows the correlation of V_{S30} with slope in Western of China. The values of V_{S30} are calculated from 1301 borehole which covers areas of three provinces, Xinjiang, Shanxi and southwest of Sichuan. It shows a clear trend of increased slope with the increased values of V_{S30}, indicating the applicability of the slope-based method.

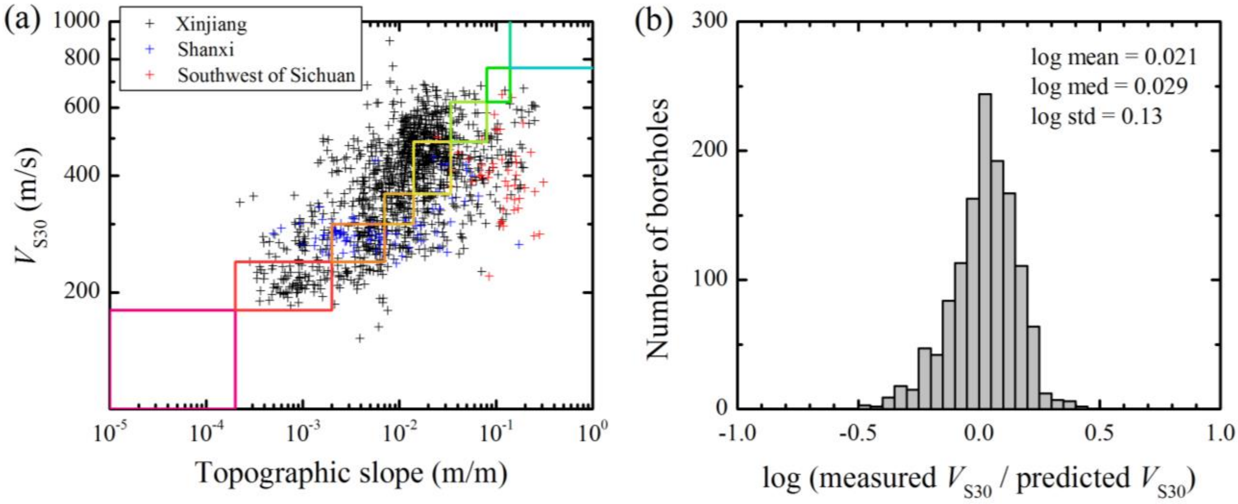

Fig. 7 – (a) Correlations of measured V_{S30} versus topographic slope for Western of China. (b) Histograms of the logarithmic differences between measured and predicted V_{S30} values. Color-coded polygons represent V_{S30} and slope ranges consistent with ranges given in Table 4s.

For a given V_{S30} range (see Table 4) the lower and upper boundaries of slope range are assigned as the values of slope corresponding to 10th and 90th percentiles of the set of V_{S30} respectively, as shown in Fig.6. To ensure the continuity of all boundaries, we make a minor adjustment subjectively. In practice the V_{S30} at any site where its topographic slope that falls within each slope range is assigned as the median value of the corresponding subdivided V_{S30} range (Fig.6; Table 4). The histograms of the logarithmic differences between measured and predicted V_{S30} values (as shown in Fig.6 (b)) imply a good prediction using the proposed proxy relationship.

Table 4 – Recommended slope range for different V_{S30} range corresponding to NEHRP site class

Site class	**V_{S30} range (m/s)**	**Slope range (m/m)**
E	< 180	< 2×10^{-4}
D	180–240	2×10^{-4}–2×10^{-3}
	240–300	0.002–0.007
	300–360	0.007–0.014
C	360–490	0.014–0.034
	490–620	0.034–0.08
	620–760	0.08–0.14
B	> 760	> 0.14

The empirical relationships between slope and V_{S30} in other region of China, and between geology and V_{S30} will be suggested in subsequent work. In our strong motion flatfile, the V_{S30} estimation will consider both the slope and geology proxies. The relative weight for each proxy will be given depending on its median and standard deviation of residuals between measured and predicted V_{S30} values. Same consideration is included in the NGA-West2 site database [18].

6. Conclusion

For the purpose to compile a strong motion flatfile in China, this study presents an overview of the collected strong ground motions in China since from 2007 to 2018, introduces briefly the architecture of the anticipated flatfile, shows the criteria of data processing and schemes for building a site database. The conclusions will be drawn as follows:

(1) More than 12, 000 strong motion recordings in China have been retrieved and these data could support adequately developing a local GMM, that motivates us to compile a strong motion flatfile.

(2) Only the most important parameters are considered to be included in this flatfile, which are classified as six categories, including event-related, source-related, station-related and waveform metadata, metrics of source-to-site distance and intensity measures.

(3) The procedures for processing the collected recordings are designed referring to those suggested by NGA-West2 project.

(4) Three schemes for evaluating site class and V_{S30} value of a strong motion station are proposed, that are measured by borehole data if it is available, predicted by an empirical relationship between site class and H/V spectral ratio, or by a proxy-based method if it is unavailable.

7. Acknowledgements

Strong-motion recordings used in this article were collected by the China Strong-Motion Network Center. Due to the current maintenance of its website (http://www.csmnc.net/) (official notice of Institute of Engineering Mechanics, CEA can be obtained at http://www.iem.ac.cn/detail.html?id=1102), we contacted the email csmnc@iem.ac.cn for data application (last accessed December 2018). The study is supported by the Scientific Research Fund of Institute of Engineering Mechanics, China Earthquake Administration (no. 2018QJGJ07), National Natural Science Foundation of China (nos. 51878632 and 51808514), and Outstanding Youth Project of Heilongjiang Natural Science Foundation (no. YQ2019E036).

8. References

[1] Ancheta TD, Darragh RB, Stewart JP, Seyhan E, Silva WJ, Chiou JBS, Wooddell KE, Graves RW, Kottke AR, Boore D.M., Kishida T., Donahue JL (2014): NGA-West 2 Database. *Earthquake Spectra,* **30** (3), 989–1005.

[2] Dawood HM, Rodriguez-Marek A, Bayless J, Goulet C, Thompson E (2016): A Flatfile for the KiK-net Database Processed Using an Automated Protocol. *Earthquake Spectra,* **32** (2), 1281–1302.

[3] Lanzano G, Sgobba S, Luzi L, Puglia R, Pacor F, Felicetta C, Amico MD, Cotton F, Bindi B (2019): The Pan-European Engineering Strong Motion (ESM) Flatfile: Compilation Criteria and Data Statistics. *Bulletin of Earthquake Engineering*, **17**(2), 561–582.

[4] Wen RZ (2016): Overview of Chinese Strong Motion Recordings, *Acta Seismologica Sinica,* **38**(4), 550–563 (in Chinese).

[5] Wang HW, Ren YF, Wen RZ (2018): Source Parameters, Path Attenuation and Site Effects from Strong-Motion Recordings of the Wenchuan Aftershocks (2008–2013) Using a Non-Parametric Generalized Inversion Technique. *Geophysical Journal International*, **212**, 872–890.

[6] Ji K, Bouaanani N, Wen RZ, Ren YF (2017): Correlation of Spectral Accelerations for Earthquakes in China. *Bulletin of the Seismological Society of America,* **107**(3), 1213–1226.

[7] Wen RZ, Xu PB, Wang HW, Ren YF (2018): Single-Station Standard Deviation Using Strong-Motion Data from Sichuan Region, China. *Bulletin of the Seismological Society of America*, **108**(4), 2237–2247.

[8] Li XJ, Zhou ZH, Huang M, Wen RZ, Yu HY, Lu DW, Zhou YN, Cui JW (2008): Preliminary Analysis of Strong-Motion Recordings from the Magnitude 8.0 Wenchuan China, Earthquake of 12 May 2008. *Seismological Research Letters*, **79**(6), 844–854.

[9] Wen RZ, Ren YF. (2014): Strong-motion observations of the Lushan Earthquake on April 20, 2013. *Seismological Research Letters*, **85**(5), 1043-1055.

[10] Xie JJ, Li XJ, Wen ZP, Wu CQ (2014): Near-Source Vertical and Horizontal Strong Ground Motion from the 20 April 2013 M_w 6.8 Lushan Earthquake in China. *Seismological Research Letters*, **85**(1), 23–33.

[11] Ren YF, Wang HW, Xu PB, Dhakal YP, Wen RZ, Ma Q, Jiang P (2018): Strong-Motion Observations of the 2017 M_s7.0 Jiuzhaigou Earthquake: Comparison with the 2013 M_s7.0 Lushan Earthquake. *Seismological Research Letters*, **89**(4), 1354–1365.

[12] Li XJ, Liu L, Wang YS, Yu T (2010): Analysis of Horizontal Strong-Motion Attenuation in the Great 2008 Wenchuan Earthquake. *Bulletin of the Seismological Society of America*, **100**(5B), 2440–2449.

[13] Kishida T, Ktenidou OJ, Darragh RB, Silva WJ (2016): Semi-Automated Procedure for Windowing Time Series and Computing Fourier Amplitude Spectra for the NGA-West2 Database. *Technical Report PEER 2016/02*, Pacific Earthquake Engineering Research, Berkeley, USA.

[14] Ji K, Ren YF, Wen RZ (2017): Site classification for National Strong Motion Observation Network System (NSMONS) stations in China using an empirical H/V spectral ratio method. *Journal of Asian Earth Sciences*, **147**, 79–94.

[15] Wald DJ and Allen TI (2007): Topographic slope as a proxy for seismic site conditions and amplification. *Bulletin of the Seismological Society of America*, **97**(5), 1379–1395.

[16] Wills CJ and Clahan KB (2006): Developing a Map of Geologically Defined Site- Condition Categories for California. *Bulletin of the Seismological Society of America*, **96**(4), 1483–1501.

[17] Yong A, Hough SE, Iwahashi J, Braverman A (2012): Terrain-Based Site Conditions Map of California with Implications for the Contiguous United States. *Bulletin of the Seismological Society of America*, **102**(1), 114–128.

[18] Seyhan E, Stewart JP, Ancheta TD, Darragh RB, Graves RW (2014): NGA-West2 Site Database. *Earthquake Spectra*, **30**(3): 1007–1024.

